

RESEARCH ARTICLE

10.1029/2018JA025762

A New Method to Retrieve Thermospheric Parameters From Daytime Bottom-Side Ne(h) Observations

L. Perrone¹ and A. V. Mikhailov²

¹Istituto Nazionale di Geofisica e Vulcanologia (INGV), Rome, Italy, ²Institute of Terrestrial Magnetism, Ionosphere and Radio-Wave Propagation (IZMIRAN), Pushkov Institute of Terrestrial Magnetism, Moscow, Troitsk, Russia

Key Points:

- A new method to extract a self-consistent set of aeronomic parameters (Tex, O, O₂, N₂, W, and EUV flux) from ionosonde observations has been proposed
- The method is applied for all seasons at middle and lower latitudes where the ionospheric F-layer is formed by solar EUV radiation
- Testing of the method on CHAMP/STAR neutral gas density has shown better accuracy than modern empirical models MSISE00, JB2008, DTM2013

Correspondence to:

L. Perrone, loredana.perrone@ingv.it

Citation:

Perrone, L., & Mikhailov, A. V. (2018). A New Method to Retrieve Thermospheric Parameters From Daytime Bottom-Side Ne(h) Observations. *Journal of Geophysical Research: Space Physics*, 123. <https://doi.org/10.1029/2018JA025762>

Received 13 JUN 2018

Accepted 28 OCT 2018

Accepted article online 5 NOV 2018

Abstract A new method to extract neutral composition (O, O₂, N₂), exospheric temperature Tex, vertical plasma drift, W, and the total solar Extreme Ultraviolet flux with $\lambda \leq 1050 \text{ \AA}$ from routine ionosonde bottom-side electron density, Ne(h), observations has been proposed. The method can be used around noontime hours for all months of the year at middle latitudes where the ionospheric F-layer is formed by solar Extreme Ultraviolet radiation. The uncertainty of the retrieved neutral gas density coincides with the announced Mean Relative Deviation $\pm(10\text{-}15\%)$ of CHAMP/STAR neutral gas density observations. The method also provides statistically significant better results in a comparison with modern Mass-Spectrometer-Incoherent-Scatter, Jacchia-Bowman 2008, and Drag Temperature Model 2013 empirical models. The thermospheric parameters retrieved for the St. Patrick Day magnetic storm and two so-called Q-disturbance periods are given as an example of the method application. The retrieved neutral gas densities for the St. Patrick Day storm are compared to Swarm-B accelerometer observations. The proposed method may be considered as a useful tool for analyses of the state of the upper atmosphere under various geophysical conditions.

1. Introduction

The Earth is surrounded by neutral atmosphere. However, our knowledge and possibilities to control the state of the upper atmosphere are much less compared to the ionosphere. This is due to the complexity of thermospheric observations. Unlike rather simple ground-based ionosonde observations of the ionosphere being conducted round o'clock for some decades, thermospheric observations are episodic and technically very complex—expensive satellite, incoherent scatter, and optical observations are required to measure thermospheric parameters. On the other hand, the state of the ionosphere reflects the state (at least at middle latitudes under sunlit conditions) of the surrounding neutral atmosphere and the intensity of solar ionizing radiation. Therefore, solving the inverse problem of aeronomy in principle, it is possible to retrieve basic thermospheric parameters (neutral composition, temperature, wind) and solar Extreme Ultraviolet (EUV) ionizing flux from ionospheric observations. This may open a way to monitor the state of the thermosphere using the worldwide ionosonde network observations (Reinisch et al., 2004).

Such attempts had been undertaken repeatedly in the past (Mikhailov, Belehaki, et al., 2012; Mikhailov & Schlegel, 1997; Oliver, 1979). The method by Oliver (1979) is designed to work only with incoherent scatter radar (ISR) data to find exospheric temperature Tex and atomic oxygen concentration. A general method to retrieve thermospheric parameters (neutral composition and Tex) and the total ionizing solar EUV flux from observed Ne(h) profile was described by Mikhailov, Belehaki, et al. (2012). However, this method is rather sophisticated for using in practice. On one hand, it requires reliable Ne(h) profiles (both in the bottom side and topside), such reliable profiles are provided only by ISR observations, the number of ISR facilities is limited and they work episodically. On the other hand, the method requires a visual control and cannot be routinely used. Recently, a new method has been proposed which uses critical frequency of F₁ layer (f_oF₁) ionosonde observations (Mikhailov & Perrone, 2016). It is simpler than the basic version (Mikhailov, Belehaki, et al., 2012) and can be used in a routine mode. However, this method is also limited being applicable only to summer months around noon hours when f_oF₁ is regularly and reliably observed. Moreover, the observed f_oF₁ should be prescribed to the height of F₁-layer maximum (h_mF₁) which normally is not known from ionosonde observations. Some approaches have been used to determine h_mF₁: (i) h_mF₁ is supposed at the height where the concentrations of atomic [O⁺] and molecular M⁺ = [NO⁺] + [O₂⁺] ions are equal, (ii) h_mF₁ is set up at the height of the inflection point or at the height of maximum (when it exists) in the calculated Ne(h) profile, (iii) h_mF₁ is

supposed at the height of the atomic oxygen ion production rate maximum (Perrone & Mikhailov, 2018). The last approach seems to provide acceptable results and it may be recommended for practical use. However, the lack of f_oF_1 observations during nonsummer months remains a serious limitation of that method. Moreover, f_oF_1 manifests a weak dependence on geomagnetic activity (Mikhailov & Schlegel, 2003) and complications may arise choosing a correct solution under disturbed conditions.

The method described in this paper is supposed to overcome the above mentioned limitations. It uses electron concentration at 180 km read from ionosonde automatically scaled Ne(h) profiles and critical frequency of F_2 layer (f_oF_2) observed by the same ionosonde. These are standard ionospheric characteristics routinely observed by modern digital ionosondes and this information is available via Internet practically in real time. The method is supposed to be applicable at middle latitudes round the year under various solar and geomagnetic conditions. Similar with the previous method by Mikhailov and Perrone (2016), only near noontime hours can be used and this is a limitation of the proposed method.

The aims of the paper may be formulated as follows.

1. To develop a method retrieving thermospheric parameters (neutral composition, exospheric temperature, meridional wind) and the total solar EUV flux with $\lambda \leq 1050 \text{ \AA}$ from observed bottom-side daytime Ne(h) profile.
2. To test the method using Challenging Minisatellite Payload/Space Three-axis Accelerometer for Research mission (CHAMP/STAR) neutral gas density observations and modern empirical thermospheric models in winter conditions when F_1 -layer is normally absent.
3. To compare the newly proposed method to the previous one based on f_oF_1 observations for summer months.
4. To demonstrate the possibilities of the new method (as an example) in an analysis of a severe St. Patrick Day ionospheric storm and some so-called Q-disturbances occurring under magnetically quiet conditions, both type of F_2 -layer disturbances being related to changes in thermospheric parameters.

2. Description of the Method

Unlike our previous method by Mikhailov and Perrone (2016), here we use electron concentration observed at F_1 -region heights (180 km) around noontime hours (10, 11, 12, 13, 14) LT and corresponding N_mF_2 values to retrieve aeronomic parameters. These concentrations (plasma frequencies at 180 km (f_{o180}) and f_oF_2) are available from worldwide digisonde observations (Reinisch et al., 2004). The fo(h) profiles are automatically scaled and they may manifest gaps and large scatter in time. From this point of view manually scaled f_oF_1 used in the previous method look more accurate and reliable considering them as input information.

Both methods have their merits and limitations. Ionosonde f_oF_1 observations are available for some decades (more than five solar cycles at some European stations) mostly for summer months and such observations can be successfully used for long-term trend analyses. Digisonde Ne(h) observations are available for a couple of decades at the best, and monthly median Ne(h) profiles which are required for trend analyses are not available. On the other hand, a possibility to retrieve thermospheric parameters for all months of the year (not only for summer ones) is an undoubted advantage of the new approach keeping in mind first of all practical aspects of the method application. However, large scatter of routinely measured plasma frequency profiles $f_o(h)$ may turn out to be a serious limitation for the new method. To illustrate this problem, Figure 1 gives a comparison of f_o at 180 km (which is in vicinity of the F_1 -layer maximum) to manually scaled f_oF_1 at Rome. Left-hand panels give examples of f_{o180} observations when point-to-point variations are not large, while right-hand panels illustrate strong f_{o180} variations. The F_1 -layer is a relatively stable formation mostly controlled by solar EUV radiation, and such strong variations of electron concentration ($Ne \propto f_{o180}^2$) in the vicinity of F_1 -layer maximum may be due to a passage of gravity waves shifting up-and-down F_1 -layer as a whole without changing f_oF_1 . Indeed, manually scaled f_oF_1 (asterisks) manifest small variations in all cases considered.

A magnetically quiet day 03 June 2006 demonstrates small f_{o180} variations, but similar quiet days 18 June 2007, 20 June 2003, and 01 July 2007 manifest large f_{o180} variations. Strong f_{o180} variations on 06 June 2006 could be related to the beginning of a geomagnetic disturbance but f_oF_1 does not demonstrate large

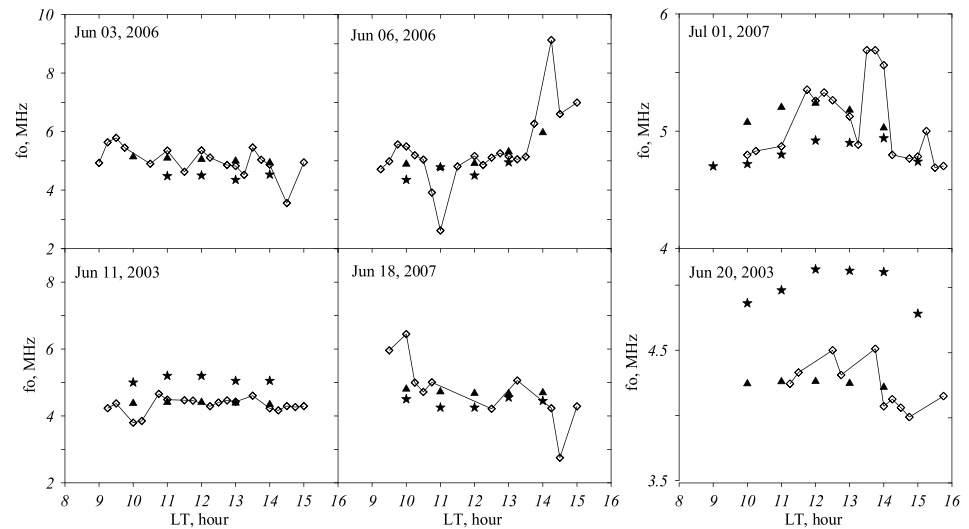


Figure 1. Examples of the automatically scaled f_o at 180 km (diamonds) in a comparison with manually scaled f_oF_1 (asterisks) variations at Rome. The final f_o smoothed variations at 180 km used as input information are given with triangles.

variations. June 11, 2003 does not show strong variations in both parameters but that was also a disturbed day. Therefore, 15-min f_o observations should be filtered and smoothed to be used in calculations. In the end we get 5 points with the final f_o values at a fixed height 180 km for (10, 11, 12, 13, 14) LT moments which are used in the retrieval process (Figure 1).

The formation mechanism of the midlatitude daytime F-layer includes photoionization of neutral [O], [O₂], [N₂] species by solar EUV with $\lambda < 1050 \text{ \AA}$, plasma transport by diffusion, and thermospheric winds and plasma recombination in the chain of ion-molecular reactions. The equations used in model calculations may be found in Mikhailov, Belehaki, et al. (2012).

We consider 5 f_{o180} values for (10, 11, 12, 13, 14) LT and noontime f_oF_2 value to find six unknowns: factors for the MSIS-86 (Hedin, 1987) model exospheric temperature T_{ex} and concentrations [O], [O₂], [N₂], vertical plasma drift, W , as well as a factor for the Nusinov (1992) model of the total solar EUV flux with $\lambda < 1050 \text{ \AA}$. Temperature T_{120} and the shape parameter S which along with T_{ex} specify the $T_n(h)$ profile (Bates, 1959) are taken from MSIS-86. An attempt to include T_{120} and S to list of unknown parameters has strongly increases the time of calculations without any noticeable changes of the final results (Perrone & Mikhailov, 2018). It should be stressed that the MSIS-86 model (Hedin, 1987) is used inside the method, while MSISE-00 (Picone et al., 2002) is used for testing and a comparison. Methods of nonlinear programming (Himmelblau, 1972) are used to extract the aeronomic parameters from ionospheric ones.

It is important to stress that thermospheric parameters (neutral composition and temperature) in the analyzed points are related by the internal structure of the MSIS-86 model, that is, spatial and temporal variations (relative variations) are given by the MSIS-86 model, we are looking for only factors to model variations to get absolute values. The same approach is applied to the EUV model by Nusinov (1992)—we are looking for a factor to the total model EUV flux but the dependence on solar activity is given by the model. Vertical plasma drift is supposed to be constant above 200 km and decreases to zero at 120 km height.

The five near noon f_{o180} values for (10, 11, 12, 13, 14) LT may be considered as independent ones. This follows from a comparison of characteristic (e-fold) times with respect to recombination to our time step of 1 hr. It is known (e.g., Rishbeth & Garriott, 1969) that daytime F₁-region is in photochemical equilibrium and may be considered to be in a quasi-stationary condition. The latter means that electron concentration at F₁-layer heights is totally controlled by the current state of the surrounding thermosphere and the intensity of the incident solar EUV radiation. For our estimates we may consider noontime conditions under deep solar minimum (15 July 2008 with $F_{10.7} = 66$, $A_p = 7$) at Rome location when half of electron concentration at 180 km is presented by atomic O⁺ ions and the other half by molecular (NO⁺ and O₂⁺) ions. Atomic ions

are converted to molecular ones via ion-molecular reactions with characteristic time $\tau_1 = 1/\beta$, where $\beta = \gamma_1[\text{N}_2] + \gamma_2[\text{O}_2]$ —linear loss coefficient. For the conditions in question, β is $\sim 6 \times 10^{-3} \text{ s}^{-1}$ resulting in $\tau_1 = 167 \text{ s}$. This is by ~ 20 times less than our 1 hr time step. The loss of molecular ions takes place via dissociative recombination with characteristic time $\tau_2 = 1/\alpha_{\text{ave}}\text{Ne}$, where $\alpha_{\text{ave}} = \alpha_1 \frac{[\text{NO}^+]}{[\text{M}^+]} + \alpha_2 \frac{[\text{O}_2^+]}{[\text{M}^+]}$ is the average-weighted dissociative recombination rate coefficient $\sim 1.4 \times 10^{-7} \text{ cm}^3/\text{s}$ and $\text{Ne} \sim 2.2 \times 10^5 \text{ cm}^{-3}$. This gives $\tau_2 \sim 30 \text{ s}$, that is, the characteristic time is by ~ 100 times less than 1 hr time step. It may be shown that the characteristic time of diffusion $\tau_{\text{dif}} = H^2/D$, where D = diffusion coefficient, $H = k(\text{Te} + \text{Ti})/m_i g$, m_i = mean molecular mass, for O_2^+ and NO^+ ions is $\sim 500 \text{ s}$, that is, it is by 17 times larger than τ_{che} .

The e-fold time for plasma drift due to thermospheric wind $\tau_{\text{drift}} = H/W \sim 5 \times 10^3 \text{ s}$ at F_1 -region heights. Thus, dissociative recombination is the controlling process at F_1 -region heights and this is a well-known result.

These estimates show that even under deep solar minimum (during solar maximum the share of molecular ions is larger at 180 km), electron concentration at 180 km is in quasi-stationary condition and five $f_{\text{O}180}$ values selected at (10, 11, 12, 13, 14) LT moments are specified by current state of the surrounding thermosphere and solar EUV radiation independently on the previous (1 hr before) value of electron concentration. The same conclusion follows from a direct comparison of the $d\text{Ne}/dt$ term to the total ion production and recombination rates in the continuity equation for electron concentration at F_1 -region heights.

However, in winter especially under solar minimum when northward thermospheric wind is strong and F_2 -layer maximum is located at $\sim 210 \text{ km}$ around noontime hours (Shubin, 2015) a downward drift of O^+ ions is possible at F_1 -layer heights. This income of O^+ ions increases to some extent electron concentration at 180 km. To take into account this downward transfer of O^+ ions, we consider $\text{Ne}(h)$ profiles in the F_2 region for all five LT moments but only observed noontime $f_{\text{O}F_2}$ is fitted during the retrieval process while other four F_2 -layer $\text{Ne}(h)$ profiles serve just as an additional source of O^+ ions for F_1 -region.

The inclusion of $f_{\text{O}F_2}$ into the retrieval process increases the number of unknowns up to six as $N_{\text{m}F_2} = 1.24 \times 10^4 (f_{\text{O}F_2})^2$ depends on vertical plasma drift, W , which is mainly related to thermospheric winds. On one the hand, $f_{\text{O}F_2}$ is a very reliable parameter routinely measured by ionospheric vertical sounding; on the other hand, $N_{\text{m}F_2}$ is very sensitive to changes in thermospheric composition and this is important considering disturbed conditions when O/N_2 ratio manifest large variations not properly predicted by empirical thermospheric models. The inclusion of $f_{\text{O}F_2}$ as a fitted parameter facilitates the process of searching for the solution, although this increases the computation time. Therefore, the proposed methods using the observed $f_{\text{O}180}$ (at 5 LT moments) and $f_{\text{O}F_2}$ (at 12 LT) provides a self-consistent set of the main aeronomic parameters responsible for the ionospheric F-region formation, namely, neutral composition (O , O_2 , N_2) and temperature T_{ex} , vertical plasma drift W (which may be converted to the effective meridional wind V_{nx}), and the total solar EUV flux with $\lambda \leq 1050 \text{ \AA}$.

3. Testing of the Method

Testing of the method is being done in two ways. At first the proposed method is compared to the initial one (Mikhailov & Perrone, 2016) based on using $f_{\text{O}F_1}$. At the second step the method is tested for winter months when $f_{\text{O}F_1}$ observations are absent but bottom-side digisonde $\text{Ne}(h)$ profiles are available. Juliusruh DPS-4 $\text{Ne}(h)$ and manually scaled $f_{\text{O}F_1}$ data for June–July of 2008, 2006, 2007, and 2003 were used to compare the old and the new methods, while Rome and Juliusruh winter DPS-4 $\text{Ne}(h)$ observations were used to test the new method. The most straightforward way to test the method is to compare the retrieved from $f_{\text{O}180}$ and from $f_{\text{O}F_1}$ neutral gas densities with the observed ones. June–July daytime CHAMP/STAR accelerometer neutral gas density observations (<http://sisko.colorado.edu/sutton/data.html>) in the European sector and Juliusruh (54.6°N; 13.4°N) ionosonde observations were used for this comparison. After the inspection of available observations at Juliusruh and by CHAMP/STAR, overall 62 dates were used to compare the two methods.

General description of solar and geomagnetic activity for the analyzed period is given by Mikhailov and Perrone (2016). Observed CHAMP/STAR neutral gas densities are reduced to the location of ionosonde station and 12 LT using MSISE-00 (Picone et al., 2002) thermospheric model and the following expression:

Table 1

Testing Results of a Newly Proposed Method in a Comparison to the Older One and Three Empirical Thermospheric Models at Juliusruh for Summer (June–July) Months of 2003–2008

Method/Model	MRD (%)	RMS (10^{-15} g/cm ³)	Bias (10^{-15} g/cm ³)
Proposed	11.6	0.478	−0.123
Retrieved (from f_oF_1)	12.8	0.590	−0.219
JB2008	14.7	0.558	0.138
MSISE00	16.7	0.621	0.225
DTM2013	17.9	0.620	0.431

Note. MRD = Mean Relative Deviation; RMS = Root-Mean-Square; MSISE00 = Mass-Spectrometer-Incoherent-Scatter; DTM2013 = Drag Temperature Model 2013; JB2008 = Jacchia-Bowman 2008.

$$\rho_{\text{station}} = \rho_{\text{CHAMP}} \frac{\text{MSISE}_{\text{station}}}{\text{MSISE}_{\text{CHAMP}}}$$

The height of CHAMP orbit decreased from ~400 km in 2003 to ~330 km in 2008 and the reduction height should be close to the satellite height to minimize possible errors of such reduction. The retrieved neutral gas density $\rho = m_1[\text{O}] + m_2[\text{O}_2] + m_3[\text{N}_2]$ does not include the contribution of [He] and [N] and the observed neutral gas densities were corrected using MSISE-00, however this correction is small ($\leq 2\%$). It should be stressed that O, O₂, N₂ concentrations are retrieved at heights of F₁ layer and then they are reduced to the height of CHAMP using the MSIS model temperature profile Tn(h) normalized by the retrieved Tex value.

Table 1 gives some statistical results of the two methods comparison: mean relative deviation, root mean square, and mean bias of the calculated neutral gas density with respect to the observed one. Three

thermospheric empirical models Mass-Spectrometer-Incoherent-Scatter (MSISE00; Picone et al., 2002), Jacchia-Bowman 2008 (JB2008; Bowman et al., 2008), and Drag Temperature Model 2013 (DTM2013; Bruinsma, 2015) were also used for a comparison.

From Table 1, it is seen that the new method based on using f_{o180} and f_oF_2 provides the best results, however they are close to those obtained with the previous method based on f_oF_1 . Looking at Bias both methods underestimate the neutral density, this could be related to slightly underestimated exospheric temperature, while the empirical models overestimate. But it should be stressed that the obtained inaccuracy of our calculations are within the absolute inaccuracy of 10–15% for CHAMP/STAR observations. Student *t*-criterion also tells us that our two methods give indistinguishable results while the difference is significant at the 97% confidence level for the JB2008 model and the difference is absolutely significant with respect to MSISE00 and DTM2013 models. Thus, one may conclude that the proposed method provides slightly better results than the old one but it manifests significantly better results compared to modern empirical models. The possibility to use it for nonsummer months may be also established by a comparison with CHAMP/STAR neutral gas density data.

A survey of available winter observations by CHAMP/STAR and DPS-4 Ne(h) profiles at Rome has given us 44 cases for testing in November, January, and February 2008. The results are given in Table 2 in a comparison with the same three thermospheric empirical models.

The results from Table 2 show us that the proposed method provides the best results, although Student *t*-criterion indicates that the difference with DTM2013 is statistically significant at the 90% confidence level only. The difference with MSISE is absolutely significant, while the difference with JB2008 is significant at the 95% confidence level. Low descriptive accuracy of the MSISE model under deep solar minimum was earlier stressed by Mikhailov, Belehaki, et al. (2012), see also the comparison results by Mehta et al. (2017).

Apart from statistical characteristics given in Table 2, a graphical presentation in a form of histograms may be also useful. We calculated the distribution of the $R = \rho_{\text{cal}}/\rho_{\text{obs}}$ ratio, where ρ_{cal} are the neutral density retrieved from the observed f_{o180} and empirical model values, while ρ_{obs} are the corresponding CHAMP/STAR measurements reduced to the ionosonde location and 12 LT. Figure 2 gives histograms of R . R_{ave} gives the average shift of the calculated ρ with respect to the observed ones. A comparison is also made with the empirical DTM2013, MSISE00, and JB2008 models. Figure 2 shows that the proposed method gives the most centered distribution with the least SD compared to the modern empirical models. Therefore, the method was shown to provide acceptable results for winter months under deep (2008) solar minimum.

To test the new method under higher levels of solar and geomagnetic activity, Juliusruh DPS-4 Ne(h) and CHAMP/SRAR observations were used for November–December 2003 and 2005, overall 49 cases were considered. November and December 2005 were magnetically quiet periods

Table 2

Testing Results of a Newly Proposed Method in a Comparison to Three Empirical Thermospheric Models at Rome for Winter Months of 2008

Method/Model	MRD (%)	RMS (10^{-15} g/cm ³)	Bias (10^{-15} g/cm ³)
Proposed	9.4	0.455	0.019
DTM2013	15.6	0.575	0.268
JB2008	20.7	0.776	0.584
MSISE00	27.5	0.905	0.793

Note. MRD = Mean Relative Deviation; RMS = Root-Mean-Square; MSISE00 = Mass-Spectrometer-Incoherent-Scatter; DTM2013 = Drag Temperature Model 2013; JB2008 = Jacchia-Bowman 2008.

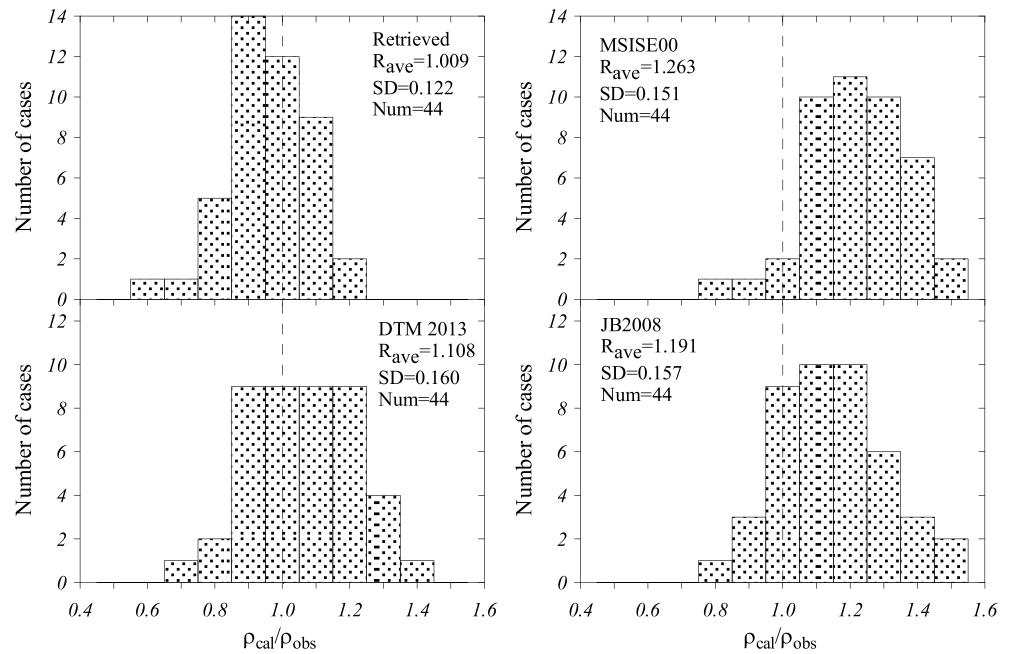


Figure 2. Distributions of $R = \rho_{cal}/\rho_{obs}$ ratio for the retrieved cases (top left panel) and those based on the DTM2013, MSISE00, and JB2008 models. Average R_{ave} , SD, and the number of analyzed cases are given. MSISE00 = Mass-Spectrometer-Incoherent-Scatter; DTM2013 = Drag Temperature Model 2013; JB2008 = Jacchia-Bowman 2008.

with monthly median $A_p < 10$ nT under a moderate level of solar activity (3-month $F_{10.7} = 86-88$), while November 2003 was a very disturbed period under 3-month $F_{10.7} \approx 138$. Only 3 of 16 considered days in November 2003 were magnetically quiet ($A_p = 6-8$ nT), while the others were strongly disturbed with A_p up to 40–60 nT and that period was analyzed separately (see section 5). Table 3 gives statistical results of the undertaken comparison. The proposed method again manifests the best results in a comparison with the three modern empirical models. The uncertainty of the retrieved neutral gas density (Tables 2 and 3) coincides with the announced absolute uncertainty $\pm(10-15\%)$ of the neutral gas density observations with the CHAMP satellite (Bruinsma et al., 2004).

The difference between the retrieved and MSISE results is statistically significant at the 99% confidence level, while the difference with JB2008 and DTM2013 models is only significant at the $\sim 90\%$ confidence level.

By analogy with testing for Rome, we are giving a graphical comparison of the obtained results (Figure 3).

The histograms in Figure 3 show that the new method provides the most centered distribution with least SD, although the JB2008 model demonstrates good results as well. Summarizing the undertaken analysis, one

may conclude that the proposed method to extract thermospheric parameters (neutral composition and temperature) from the observed electron concentration at 180 km and $N_m F_2$ around noontime hours manifests an acceptable accuracy in a comparison with CHAMP/STAR neutral gas density observations and modern empirical thermospheric models.

Table 3

Testing Results of a Newly Proposed Method in a Comparison to Three Empirical Thermospheric Models at Juliusruh for November–December of 2003 and 2005

Method/Model	MRD (%)	RMS (10^{-15} g/cm ³)	Bias (10^{-15} g/cm ³)
Proposed	13.1	0.591	−0.044
JB2008	16.4	0.831	0.292
DTM2013	19.2	0.753	0.325
MSISE00	22.6	0.923	0.530

Note. MRD = Mean Relative Deviation; RMS = Root-Mean-Square; MSISE00 = Mass-Spectrometer-Incoherent-Scatter; DTM2013 = Drag Temperature Model 2013; JB2008 = Jacchia-Bowman 2008.

4. Some Examples of the Method Application

The developed method to extract thermospheric parameters from the observed bottom-side Ne(h) distribution opens wide possibilities for aeronomic investigations. Some examples are given below with the method applied to an analysis of a strong ionospheric storm on 17–19 March 2015—the so-called St. Patrick’s Day magnetic storm and to negative and positive Q-disturbances (Mikhailov et al., 2004) which take place

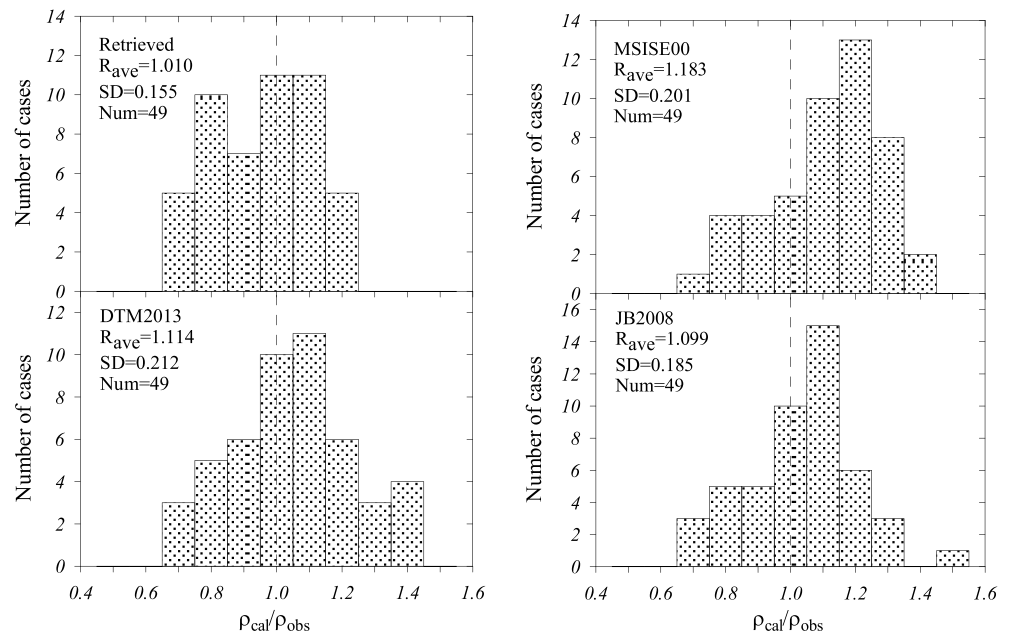


Figure 3. Distributions of $R = \rho_{\text{cal}}/\rho_{\text{obs}}$ ratio for the retrieved neutral gas density (top left panel) and those based on the DTM2013, MSISE00, and JB2008 models. Average R_{ave} , SD, and the number of analyzed cases are given. MSISE00 = Mass-Spectrometer-Incoherent-Scatter; DTM2013 = Drag Temperature Model 2013; JB2008 = Jacchia-Bowman 2008.

under magnetically quiet conditions. The 17–19 March 2015 was an isolated severe storm with AE index reaching 1,570 nT and 3-hr ap index up to 179 nT on 17 March. A detailed analysis of this storm using model simulations may be found in Dmitriev et al. (2017). We have considered three ionosonde stations to illustrate the possibilities of the proposed method: Moscow, Juliusruh, and Rome where DPS-4 observations provide necessary input information. Moscow ($\Phi = 51.1$) and Juliusruh ($\Phi = 53.9$) have close geomagnetic latitudes and should manifest similar variations both in ionospheric and thermospheric parameters, while Rome ($\Phi = 41.8$) is a lower latitude station and storm variations in all parameters should be different. Figure 4 gives variations of AE and ap-3 hr indices and corresponding f_oF_2 variations in a comparison with monthly medians at the three stations.

March 16 was a quiet day with f_oF_2 variations close to monthly median ones. The first splash of auroral activity at 06–09 UT on 17 March with the AE index increase up to 778 nT produced a well-pronounced positive phase in f_oF_2 on the three stations close on time at Moscow and Juliusruh and with some delay at Rome indicating the TAD origin of this effect. The positive f_oF_2 storm phase was immediately followed by a pronounced negative one clearly seen at Moscow and Juliusruh but not at Rome where the positive storm effect was on until nighttime hours. Strong negative storm effects took place during both daytime and nighttime hours on 18–19 March. At Rome negative f_oF_2 deviations are mainly seen only during nighttime hours when the background equatorward thermospheric circulation shifted the disturbed neutral composition from higher to lower latitudes. Therefore, that was a classic two-phase storm effect normally taking place when a severe storm SC takes place during daytime hours (Mikhailov, Perrone, et al., 2012). The mechanism of such storms is related to changes in the thermospheric circulation with corresponding changes in neutral composition (Prölss, 1995, 2004).

An interesting effect may be noted in relation with this storm case. On 19 March, the magnetic storm still was in progress, a strong negative F_2 -layer storm effects took place at Moscow and Juliusruh during both nighttime and daytime hours (Figure 4). At Rome, negative deviations took place only during nighttime, while f_oF_2 were close to median values during daytime hours. The disturbed neutral composition was expected at Rome on 19 March as well because the geomagnetic storm was still in progress, however this is not seen in f_oF_2 variations. This is a well-known morphological feature when in the course of a storm f_oF_2 values may turn out to be close to the median for several hours (Danilov, 2001).

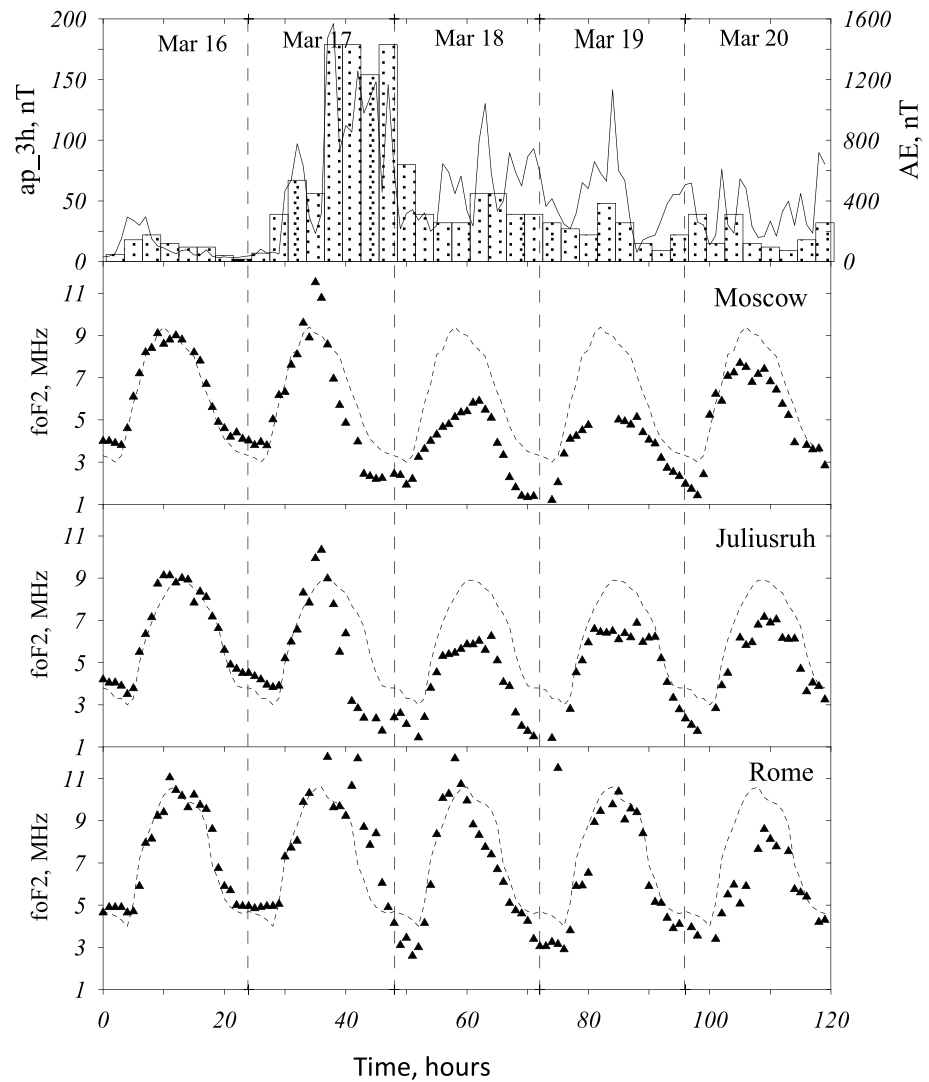


Figure 4. Observed hourly and monthly median (dashes) f_oF_2 variations at Moscow, Juliusruh, and Rome for the 16–20 March 2015 geomagnetic storm. Observed 3-hr ap and hourly AE (solid line) indices are shown in the top panel.

Let us check if our method to extract thermospheric parameters confirms the present-day mechanism of mid-latitude F_2 -layer storms. Unfortunately, we cannot follow the development of this process in time as we can analyze only daily (at 12 LT) variations. The main thermospheric parameters and h_mF_2 retrieved from the observed ionospheric observations are listed in Table 4.

The obtained results (Table 4) confirm the upsurge of the equatorward wind V_{nx} (positive $W = V_{nx}\sin\lambda\cos\lambda$ up to 36 m/s) related to the increase of auroral heating on 17 March. According to the F_2 -layer storm mechanism (e.g., Prölss, 2004) the enhanced equatorward wind is followed by the disturbed thermospheric composition with low $[O]/[N_2]$ ratio. Our results indicate a strong $[O]/[N_2]_{300}$ decrease on 17 March clearly seen at the three stations. Despite this $[O]/[N_2]_{300}$ decrease, a pronounced positive F_2 -layer storm phase takes place at the stations in question (Figure 4) and this may be only related to a strong equatorward wind (Table 4) generated by auroral heating. A decreased $[O]/[N_2]_{300}$ ratio is kept on 18–20 March and this is presumably due to the transfer of the disturbed neutral composition from the auroral zone during nighttime hours when the thermospheric wind is equatorward one. This results in nighttime negative F_2 -layer disturbances well-seen at Moscow and Juliusruh and to a less extent at Rome. Strong negative f_oF_2 disturbances at Moscow and Juliusruh also take place during daytime hours (Figure 4), and this may be attributed to low $[O]/[N_2]_{300}$ ratio on 18–20 March (Table 4). At lower latitude station, Rome f_oF_2 daytime negative storm effects are not

Table 4
Retrieved Exospheric Temperature, T_{ex} , Concentration of Atomic Oxygen, [O], and [O]/[N₂] Ratio at 300 km as well as Vertical Plasma Drift, W at Moscow, Juliusruh, and Rome for 12 LT of 16–20 March 2015

Moscow					
Parameter	16 March	17 March	18 March	19 March	20 March
T_{ex} , K	992	1151	1125	1016	995
[O] _{300C} , cm ⁻³	6.34	5.92	6.04	4.81	5.10
[O]/[N ₂] ₃₀₀	5.48	2.00	2.34	3.04	4.00
W, m/s	-14.7	31.0	-16.7	-16.1	-16.1
$h_m F_2$, km	250	368	266	248	250
Juliusruh					
T_{ex} , K	1004	1187	1158	1031	1018
[O] ₃₀₀ ×10 ⁸ , cm ⁻³	6.24	5.72	6.02	4.78	4.64
[O]/[N ₂] ₃₀₀	5.20	1.84	2.21	3.29	3.26
W, m/s	-10.8	35.9	-14.2	-19.9	-18.4
$h_m F_2$, km	265	376	271	246	248
Rome					
T_{ex} , K	1010	1203	1151	1033	1037
[O] ₃₀₀ ×10 ⁸ , cm ⁻³	7.10	5.65	8.64	6.83	5.31
[O]/[N ₂] ₃₀₀	6.05	2.00	3.84	5.03	3.66
W, m/s	-9.8	27.6	-0.1	-8.8	-20.0
$h_m F_2$, km	267	378	320	272	252

pronounced on 18–19 March as the [O]/[N₂]₃₀₀ decrease is not that large as at higher latitude stations. Moreover, the thermospheric parameters (T_{ex} , [O], [O]/[N₂]) and W were close to quiet time values on 16 March (Table 4) and this explains the closeness of $f_o F_2$ variations to median ones (Figure 4). In the end daytime $f_o F_2$ negative disturbance has appeared at Rome on 20 March as well (Figure 4). The crucial factor was an increase of the poleward V_{nx} under a relatively low [O]/[N₂]₃₀₀ ratio (Table 4) resulting in a decrease of $h_m F_2$ with the corresponding increase of the recombination rate. Therefore, the retrieved thermospheric parameter variations agree with the present-day understanding of F₂-layer storms at middle latitudes under strong geomagnetic activity.

The reality of the retrieved thermospheric parameters for the analyzed period was checked by a comparison with neutral gas density observations. Swarm-B accelerometer data provide such an opportunity. The retrieved neutral gas densities at Juliusruh, Rome, and Moscow were reduced to the Swarm-B orbits using the MSISE00 model (Picone et al., 2002). Table 5 gives the retrieved and observed neutral gas densities for 16–20 March 2015. Mean of three orbit points with latitudes of observations close to the latitude of an ionosonde were used in Table 5.

Table 5
Observed by Swarm-B and Retrieved at the Three Stations Neutral Gas Densities for the St. Patrick Day Storm Period

Moscow					
Density (10 ⁻¹⁶ g/cm ³)	16 March	17 March	18 March	19 March	20 March
Observed	3.916	6.144	7.568	4.353	3.754
Retrieved	3.494	5.664	6.181	3.277	3.417
Difference (%)	10.7	7.8	18.3	24.7	9.0
Juliusruh					
Observed	4.014	6.052	7.569	3.837	3.860
Retrieved	3.793	6.840	6.513	3.185	3.200
Difference (%)	5.5	13.0	13.9	17.0	17.1
Rome					
Observed	4.224	5.839	7.876	3.734	3.909
Retrieved	4.167	6.354	8.431	4.258	3.698
Difference (%)	1.5	8.8	7.1	14.1	5.4

Note. Differences between observed and retrieved values are given in the third lines. The retrieved densities were reduced to height, latitude, longitude, and UT of the Swarm-B orbit.

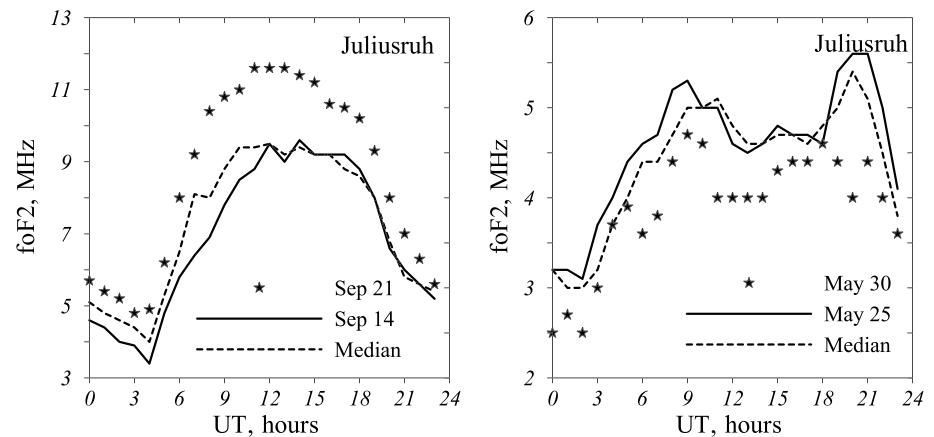


Figure 5. Positive on 21 September 2002 and negative on 30 May 2009 Q-disturbances along with monthly median and reference diurnal f_oF_2 variations observed at Juliusruh.

Table 5 shows that the retrieved neutral densities follow the observed ones with an acceptable accuracy. Higher latitude stations Moscow and Juliusruh manifest larger deviations than Rome. It should be mentioned that the absolute accuracy of Swarm neutral gas density observations has not been officially announced yet but an uncertainty of $\pm 15\%$ can be accepted as a reasonable one. For the quiet day of 16 March and the most disturbed day of 17 March with $A_p = 108$ the difference between observed and retrieved neutral gas densities is $\leq 13\%$. These results may be considered as an additional test of the proposed method indicating the reality of the retrieved aeronomic parameters for the St. Patrick Day storm period.

There are also F_2 -layer perturbations which occur under very low geomagnetic activity, the so-called Q-disturbances (Mikhailov et al., 2004). Their origin and mechanisms are still being discussed (e.g., Chen et al., 2017). Obviously, that such Q-disturbances also reflect the corresponding changes in the thermospheric parameters (neutral composition, temperature, winds) and the proposed method can be very useful for their analysis. Q-disturbances are frequent in the nighttime but they are not numerous during daytime (especially negative ones). Two such daytime cases were found at Juliusruh: a positive Q-disturbance on 21 September 2002 and a negative one on 30 May 2009. In both cases, 3-hr a_p indices were ≤ 7 for the previous 24-hr period. Variations of f_oF_2 on 14 September 2002 and 25 May 2009 which are close to monthly median f_oF_2 were chosen as the reference days. The observed f_oF_2 variations for the analyzed periods are given in Figure 5.

The retrieved aeronomic parameters along with observed N_mF_2 for the two periods at 12 LT are given in Tables 6 and 7.

In accordance with the mechanism of daytime positive and negative Q-disturbances (Mikhailov et al., 2007) the thermospheric circulation and related with it atomic oxygen concentration variations are responsible for the observed effect. The positive N_mF_2 Q-disturbance on 21 September is due to larger atomic oxygen concentration and smaller downward plasma drift compared to the reference day 14 September (Table 5). Smaller W corresponds to smaller northward solar-driven thermospheric wind. Larger $[O]$ and smaller W result in larger h_mF_2 on 21 September (Table 5). The situation with the negative Q-disturbance on 30 May is quite opposite to the previous one. Smaller atomic oxygen concentration and larger downward plasma

Table 6
Retrieved Temperature T_{ex} , Atomic Oxygen $[O]$ at 300 km, Vertical Plasma Drift W Along With h_mF_2 and N_mF_2 for the Positive Q-Disturbance Day 21 September 2002 and for the Reference Day 14 September 2002

Date	T_{ex} , K	$[O]_{300} \times 10^8$, cm^{-3}	W , m/s	h_mF_2 , km	$N_mF_2 \times 10^5$, cm^{-3}
21 September	1125	9.04	-0.5	310	16.1
14 September	1199	8.68	-9.6	290	9.82

Table 7

Retrieved Temperature T_{ex} , Atomic Oxygen $[O]$ at 300 km, Vertical Plasma Drift W Along With $h_m F_2$ and $N_m F_2$ for the Negative Q-disturbance Day 30 May 2009 and for the Reference Day 25 May 2009

Date	T_{ex} , K	$[O]_{300} \times 10^8, \text{cm}^{-3}$	W , m/s	$h_m F_2$, km	$N_m F_2 \times 10^5, \text{cm}^{-3}$
30 May	819	2.07	-7.0	220	2.19
25 May	812	2.48	-1.7	236	2.98

drift on 30 May compared to 25 May result in lower $h_m F_2$ and smaller $N_m F_2$ on 30 May (Table 6). Therefore, the method based on quite different principles confirms the earlier obtained results on the Q-disturbances formation mechanism.

5. Discussion

The proposed method seems to open a real possibility to analyze the state of the upper atmosphere using routine ground-based ionosonde observations when bottom-side $N_e(h)$ profiles are available. Naturally, the method has its own limitations: it can be only applied at middle latitudes around noontime hours when the ionosphere is formed by solar EUV radiation.

Another serious limitation is related to using $N_e(h)$ profiles. Such data are provided only by modern digi-sondes like DPS-4 but the period with available observations covers a couple of decades at the best. This means that the method cannot be used for long-term trend analyses as $N_e(h)$ historical observations are absent. However, the method may be changed to use available historic $f_o F_2$ and $f_o F_1$ data instead of $f_o F_{180}$ observations for summer months.

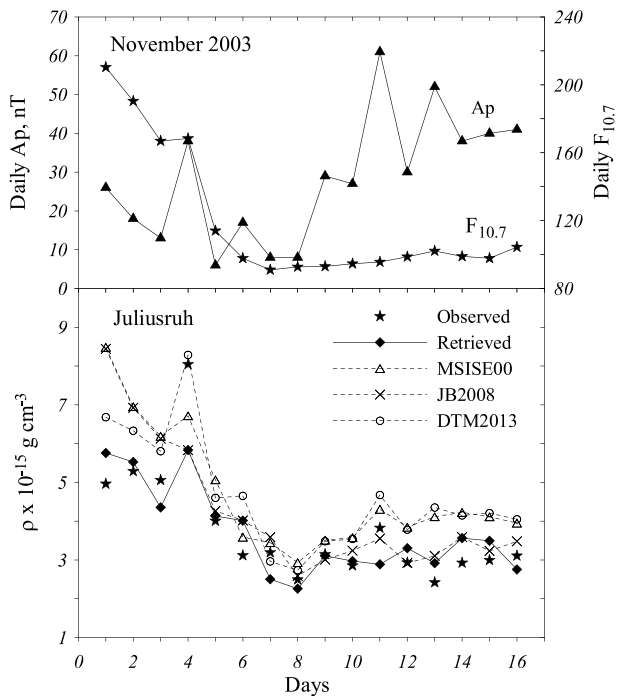


Figure 6. Solar and geomagnetic activity variations in November 2003 (top panel) and the observed by Challenging Minisatellite Payload/Space Three-axis Accelerometer for Research mission neutral gas density along with the retrieved and model ρ variations (bottom panel). MSISE00 = Mass-Spectrometer-Incoherent-Scatter; DTM2013 = Drag Temperature Model 2013; JB2008 = Jacchia-Bowman 2008.

Unlike empirical thermospheric models which are driven by global indices of solar and geomagnetic activity, the proposed method is based on local $N_e(h)$ observations in the daytime F-region. Electron concentration reflects the current state of the surrounding thermosphere and the incident solar EUV flux and may be considered as a sensitive indicator to monitor the state of the upper atmosphere in the vicinity of working ionosonde. This was shown by a direct comparison with the excellent CHAMP/STAR neutral gas density observations. The obtained inaccuracy of the retrieved ρ was shown to coincide with the absolute uncertainty $\pm(10-15\%)$ of the neutral gas density observations with the CHAMP satellite (Bruinsma et al., 2004), while modern empirical thermospheric models demonstrate as a rule lower accuracy (Table 1–3). It was shown that the difference with empirical models is statistically significant, therefore the results obtained with the proposed method may be considered as reliable.

To demonstrate possible applications of the developed method, the St. Patrick Day storm period and two Q-disturbance cases were analyzed using European ionosonde observations. The retrieved thermospheric parameter manifests variations which agree with the present-day theory of the disturbed F_2 -layer. Swarm-B neutral gas density observations provide a possibility to compare these observations to our results for the St. Patrick Day storm period. The undertaken comparison has shown that the retrieved neutral gas densities are in a reasonable agreement with the observations (Table 5). It should be mentioned that the absolute uncertainty of Swarm neutral gas density observations has not been officially announced yet but one may hope that it is not worse than $\pm(10-15\%)$ manifested by CHAMP/STAR.

It is interesting to understand the possibilities of the proposed method under extreme geophysical conditions. A good example presents the period of November 2003 when during some days solar activity fell

down from $F_{10.7} = 210$ to 91 and geomagnetic activity varied from quiet level ($A_p = 6-8$) up to $A_p = 61$ (Figure 6). This period was earlier considered during our checking of winter conditions but here for a better obviousness we are giving a plot to compare the retrieved neutral gas density to the observed one and empirical model values.

During the first 4 days of November when solar activity was very high all empirical models strongly overestimate the observed neutral gas density, while the proposed method based on the observed electron concentration gives ρ close to the observed values. After 9 November under elevated geomagnetic activity MSISE00 and DTM2013 also overestimate the observed neutral gas density while the retrieved ρ values are close to observed ones. It is interesting to note that JB2008 also demonstrates good results for this magnetically disturbed period. A good accuracy of this model was earlier stressed within the CEDAR project (Shim et al., 2012).

Therefore, the proposed method basing on local Ne(h) observations rather than on global indices of solar and geomagnetic activity used by empirical models can give more precise information on the state of the thermosphere overhead, of course with all earlier mentioned reservations.

We have not discussed the retrieved vertical plasma drifts as such analysis requires simultaneous ISR and digisonde observations. Such possibility exists at Millstone-Hill but a separate paper should be devoted to such analysis. We have not also discussed the retrieved solar EUV fluxes. On one hand, we have already presented and discussed our results on EUV earlier (Mikhailov et al., 2017; Mikhailov & Perrone, 2018); on the other hand, this topic should be considered in relation with any geophysical problem, while this paper is devoted to the method and its testing using reliable CHAMP/STAR neutral gas density observations.

6. Conclusions

The results of undertaken analysis may be formulated as follows.

1. A new method to extract neutral composition (O , O_2 , N_2), exospheric temperature T_{ex} , vertical plasma drift W , and the total solar EUV flux with $\lambda \leq 1050 \text{ \AA}$ from routine bottom-side Ne(h) observations has been proposed. The input parameters are electron concentration at 180 km height and f_oF_2 around noontime hours as well as standard solar ($F_{10.7}$) and geomagnetic (A_p) activity indices. The method can be used around noontime hours at middle latitudes where the ionospheric F-layer is formed by solar EUV radiation.
2. Unlike the previous version of the method by Mikhailov and Perrone (2016), which was confined by summer months when f_oF_1 are reliably detected on ionograms, the proposed method can be used round the year when fo_{180} and f_oF_2 are available. A comparison of the new method to the previous one for summer months (overall 62 cases) has shown that they demonstrate the same accuracy in a comparison with CHAMP/STAR neutral gas density observations.
3. Testing of the new method on winter CHAMP/STAR observations in 2003, 2005, and 2008 (overall 93 cases) has shown that the proposed method provides better accuracy than modern empirical models MSISE00, JB2008, and DTM2013, the difference being statistically significant.
4. The uncertainty of the retrieved neutral gas density coincides with the announced absolute uncertainty $\pm(10-15\%)$ of the neutral gas density observations with the CHAMP/STAR (Bruinsma et al., 2004).
5. An application of the developed method to European ionospheric observations during the St. Patrick Day magnetic storm (17–20 March 2015) and two periods with negative and positive Q-disturbances (30 May 2009 and 23 September 2002) have shown that the retrieved neutral composition, exospheric temperature, and vertical plasma drifts (related to thermospheric winds) demonstrate variations which are in agreement with the present-day understanding of F_2 -layer storm-time variations at middle latitudes.
6. The retrieved neutral gas densities at Moscow, Juliusruh, and Rome for the St. Patrick Day magnetic storm period were shown to be in an acceptable agreement with Swarm-B observations confirming the reality of the retrieved aeronomic parameter variations.
7. Therefore, the developed method may be considered as a useful tool for analyses of the state of the upper atmosphere using routinely observed bottom-side Ne(h) profiles. The method provides a self-consistent set of the main aeronomic parameters responsible for the formation of the ionospheric F-layer at middle latitudes around noontime hours.

Acknowledgments

The authors thank the European Space Agency that have supported this research in the frame of the SAFE Project (Contract 4000116832/15/NL/MP) under the STSE (Support To Science Element). The Juliusruh data are kindly provided by Leibniz institute of Atmospheric Physics - Field station Juliusruh, Germany. The authors also thank the Lowell DIDBase through GIRO to provide ionospheric data and GFZ German Research Center for CHAMP data (ftp://anonymous@isdctftp.gfz-potsdam.de/champ/). The Rome data are provided by Istituto Nazionale di Geofisica e Vulcanologia (http://www.eswua.ingv.it/).

References

Bates, D. R. (1959). Some problems concerning the terrestrial atmosphere above the 100 km level. *Proceedings of the Royal Society of London Series A*, 253, 451–462. <https://doi.org/10.1098/rspa.1959.0207>

Bowman, B.R., Tobiska, W.K., Marcos, F.A., Huang, C.Y., Lin, C.S., & Burke W.J. (2008). A new empirical thermospheric density model JB2008 using new solar and geomagnetic indices, AIAA/AAS Astrodynamics Specialist Conference 18–21 August 2008, Honolulu, Hawaii, paper paper AIAA 2008–6438 (19pp), 2008, http://ccar.colorado.edu/muri/AIAA_2008-6438_JB2008_Model.pdf

Bruinsma, S. (2015). The DTM-2013 thermosphere model. *Journal of Space Weather and Space Climate*, 5, A1. <https://doi.org/10.1051/swsc/2015001>

Bruinsma, S., Tamagnan, D., & Biancale, R. (2004). Atmospheric density derived from CHAMP/STAR accelerometer observations. *Planetary and Space Science*, 52, 297–312. <https://doi.org/10.1016/j.pss.2003.11.004>

Chen, Z., Wang, J.-S., Deng, X., Deng, Y., Huang, C.-M., Li, H. M., & Wu, Z. X. (2017). Study on the relationship between the residual 27 day quasi-periodicity and ionospheric Q disturbances. *Journal of Geophysical Research: Space Physics*, 122, 2542–2550. <https://doi.org/10.1002/2016JA023195>

Danilov, A. D. (2001). F-2 region response to geomagnetic disturbances. *Journal of Atmospheric and Solar - Terrestrial Physics*, 63, 441–449. [https://doi.org/10.1016/S1364-6826\(00\)00175-9](https://doi.org/10.1016/S1364-6826(00)00175-9)

Dmitriev, A. V., Suvorova, A. V., Klimenko, M. V., Klimentko, V. V., Ratovsky, K. G., Rakhmatulin, R. A., & Parkhomov, V. A. (2017). Predictable and unpredictable ionospheric disturbances during St.Patrick's Day magnetic storms of 2013 and 2015 and on 8–9 March 2008. *Journal of Geophysical Research: Space Physics*, 122, 2398–2423. <https://doi.org/10.1002/2016JA023260>

Hedin, A. E. (1987). MSIS-86 thermospheric model. *Journal of Geophysical Research*, 92, 4649–4662. <https://doi.org/10.1029/JA092iA05p04649>

Himmelblau, D. M. (1972). *Applied nonlinear programming*. New York: McGraw-Hill Book Company.

Mehta, P. M., Walker, A. C., Sutton, E. K., & Godinez, H. C. (2017). New density estimates derived using accelerometers on board the CHAMP and GRACE satellites. *Space Weather*, 15, 558–576. <https://doi.org/10.1002/2016SW001562>

Mikhailov, A., & Schlegel, K. (1997). Self-consistent modelling of the daytime electron density profile in the ionospheric F-region. *Annales Geophysicae*, 15, 314–326. <https://doi.org/10.1007/s005850050446>

Mikhailov, A. V., Belehaki, A., Perrone, L., Zolesi, B., & Tsagouri, I. (2012). Retrieval of thermospheric parameters from routine ionospheric observations: Assessment of method's performance at mid-latitudes daytime hours. *Journal of Space Weather and Space Climate*, 2, A03. <https://doi.org/10.1051/swsc/2012002>

Mikhailov, A. V., Depuev, V. H., & Depueva, A. H. (2007). Synchronous NmF2 and NmE daytime variations as a key to the mechanism of quiet-time F2-layer disturbances. *Annales Geophysicae*, 25, 483–493. <https://doi.org/10.5194/angeo-25-483-2007>

Mikhailov, A. V., Depueva, A. K., & Leschinskaya, T. Y. (2004). *International Journal of Geomagnetism and Aeronomy*, 5, 1–14. <https://doi.org/10.1029/2003GI000058>

Mikhailov, A. V., & Perrone, L. (2016). Geomagnetic control of the midlatitude daytime foF1 and foF2 long-term variations: Physical interpretation using European observations. *Journal of Geophysical Research: Space Physics*, 121, 7193–7203. <https://doi.org/10.1002/2016JA022716>

Mikhailov, A. V., & Perrone, L. (2018). Interminimum foF1 differences and their physical interpretation. *Journal of Geophysical Research: Space Physics*, 123, 768–780. <https://doi.org/10.1002/2017JA024831>

Mikhailov, A. V., Perrone, L., & Nusinov, A. A. (2017). A mechanism of midlatitude noontime f_oE long-term variations inferred from European observations. *Journal of Geophysical Research: Space Physics*, 122, 4466–4473. <https://doi.org/10.1002/2017JA023909>

Mikhailov, A. V., Perrone, L., & Smirnova, N. V. (2012). Two types of positive disturbances in the daytime mid-latitude F2-layer: Morphology and formation mechanisms. *Journal of Atmospheric and Solar - Terrestrial Physics*, 81–82, 59–75. <https://doi.org/10.1016/j.jastp.2012.04.003>

Mikhailov, A. V., & Schlegel, K. (2003). Geomagnetic storm effects at F₁-layer heights from incoherent scatter observations. *Annales Geophysicae*, 21, 583–596. <https://doi.org/10.5194/angeo-21-583-2003>

Nusinov, A.A. (1992). Models for prediction of EUV and X-ray solar radiation based on 10.7-cm radio emission., Proc. Workshop on Solar Electromagnetic Radiation for Solar Cycle 22, Boulder, Co., July 1992, Ed. R.F. Donnelly, NOAA ERL. Boulder, Co., USA, 354–359.

Oliver, W. L. (1979). Incoherent scatter radar studies of the daytime middle thermosphere. *Annales de Geophysique*, 35, 121–139.

Perrone, L., & Mikhailov, A. V. (2018). Reply to comments by S. Zhang, J.M. Holt, P.J. Erickson, and L.P. Goncharenko on the paper “Long-term variations of exospheric temperature inferred from foF1 observations: A comparison to ISR Ti trend estimates” by L. Perrone and A.V. Mikhailov. *Journal of Geophysical Research: Space Physics*, 123. <https://doi.org/10.1029/2017JA025039>

Picone, J. M., Hedin, A. E., Drob, D. P., & Aikin, A. C. (2002). NRLMSISE-00 empirical model of the atmosphere: Statistical comparison and scientific issues. *Journal of Geophysical Research*, 107(A12), 1468. <https://doi.org/10.1029/2002JA009430>, SIA 15-1–SIA 15-16

Prölss, G. W. (2004). *Physics of the Earth's space environment (An introduction)*, (p. 513). Berlin Heidelberg: Springer-Verlag. <https://doi.org/10.1007/978-3-642-97123-5>

Prölss, G. W. (1995). In Volland (Ed.), *Ionospheric F-region storms, handbook of atmospheric electrodynamics*, (Vol. 2, pp. 195–248). Boca Raton: CRC Press.

Reinisch, B. W., Galkin, I. A., Khmyrov, G., Kozlov, A., & Kitrosser, D. F. (2004). Automated collection and dissemination of ionospheric data from the digisonde network. *Advances in Radio Science*, 2, 241–247.

Rishbeth, H., & Garriott, O. K. (1969). *Introduction to ionospheric physics*. New York and London: Academic Press.

Shim, J. S., Kuznetsova, M., Rastatter, L., Bilitza, D., Butala, M., Codrescu, M., et al. (2012). CEDAR Electrodynamic Thermosphere Ionosphere (ETI) Challenge for systematic assessment of ionosphere/thermosphere models: Electron density, neutral density, NmF2, and hmF2 using space based observations. *Space Weather*, 10, S10004. <https://doi.org/10.1029/2012SW000851>

Shubin, V. N. (2015). Global median model of the F2-layer peak height based on ionospheric radio-occultation and ground-based Digisonde observations. *Advances in Space Research*, 56(5), 916–928. <https://doi.org/10.1016/j.asr.2015.05.029>